VIII Minsk International Seminar "Heat Pipes, Heat Pumps, Refrigerators, Power Sources",
Minsk, Belarus, September 12–15, 2011

NON INTRUSIVE MEASUREMENT OF THE MASS FLOW RATE INSIDE A CLOSED LOOP TWO-PHASE THERMOSYPHON

Bruno Agostini, Eva Ferreira
ABB Ltd. Switzerland,
Corporate Research,
Segelhofstrasse 1K,
5405 Daettwil, Switzerland
Phone: +41 (0)58 586 80 42
Telefax: +41 (0)58 586 40 06
Bruno.agostini@ch.abb.com

Abstract

Two-phase cooling is a promising technology for electronics cooling. It allows using dielectric fluids in passive systems and benefit from high heat transfer coefficients. Thermosyphons are a particularly interesting technology in the field of power electronics being entirely passive and simple equipments. Their performances are strongly related to the flow rate of the fluid inside the thermosyphon. In mini-channels thermosyphons liquid entrainment occurs so that flow rate is difficult to evaluate, hence the need for a non intrusive measurement method. For this purpose a mini-channel thermosyphon was manufactured out of borosilicate glass and equipped with a semi-transparent ITO layer as a direct current heating evaporator. It was illuminated by two lasers through the glass tube and the voltage from two photodiodes placed on the opposite side was measured. With an appropriate signal processing the maximal velocity was determined together with length and frequency of the vapor bubbles, the frequency of the thermosyphon cycle for several filling ratios and for various heating powers. From these measurements the total mass flow rate, the liquid mass flow rate, the gas mass flow rate, the void fraction, the vapor quality and the flow cycle frequency were calculated and compared to a thermosyphon simulation model developed at ABB.

KEYWORDS
Two-phase cooling, thermosyphon, bubble velocity, laser, photodiode.

INTRODUCTION

Thermosyphon cooling systems have been recognized to be beneficial for thermal management of electronics. The use of dielectric fluids and pumpless operation altogether with high heat transfer coefficients is an attractive combination for power electronics thermal management. In a state-of-the art Vasiliev [1] described the use of heat pipes for power semiconductors cooling, highlighting that it allows for higher power density. Thermosyphons using small channels are particularly appealing for their compactness and low material and fluid use. However, very few experimental data or models are available with the new dielectric fluids at the required working temperatures and channel diameters. Still, available studies on different thermosyphon configurations are helpful to outline some trends. Furthermore, small diameter channels allow taking advantage of the so called bubble pump effect to further increase the performances of the thermosyphon. This effect causes liquid plugs to be propelled in the channels and delay dry-out phenomena. This liquid pushing effect typically shows a maximum with heat load as shown by Delano [2]. An issue in such system is the flow instabilities, all the more so that the channel diameter decreases. Nayak *et al* [3] conducted a numerical study of boiling flow instability of a reactor thermosyphon system and showed that increasing the riser diameter, high power Type {II} instabilities disappear but a low power, low quality Type {I} instabilities appear. The effects of subcooling and riser length were also studied. The performances of a two-phase thermosyphon loop with a small diameter channel evaporator have been recently measured by Khodabandeh [4, 5]. The evaporator channels diameter ranged from 1.1 to 3.5 mm, but the riser had a diameter of 6.1 mm. The heat transfer coefficient was found to be strongly dependant on heat flux and the pressure drop to be adequately predicted by the homogeneous model. The influence of the filling ratio is also a crucial parameter. Ong and Haider-E-Alahi [6] investigated this effect on a R134a filled thermosyphon and

found that the performances increased with the filling ratio, reaching a maximum at about 0.8. Abou-Ziyan *et al* [7] found a maximal performance at a filling ratio of 0.5, also with a R134a filled thermosyphon. Furthermore they showed that vibrations could act against the boiling limit and extend the operating range of the thermosyphon. MacDonald *et al* [8] measured experimentally an optimum at 35% of filling ratio with refrigerant R11 in a large diameter tube two-phase thermosyphon and also showed with a numerical model that this optimum was strongly dependent on the respective lengths of the evaporator, riser and condenser. This last fact might explain why Ong and Haider-E-Alahi [6] and Abou-Ziyan *et al* [7], having different evaporator, riser and condenser lengths, found different optimal filling ratios. The Present study will highlight the effects of filling on mass flow and instabilities in the thermosyphon.

EXPERIMENTAL SETUP

The principle of the thermosyphon and the experimental setup are shown in Fig. 1. The thermosyphon is filled with a low global warming potential fluid (Novec 649). At the bottom left of the system, an evaporator heats up the fluid beyond the onset of nucleate boiling thus generating vapor bubbles. Then, these elongated and confined bubbles grow, pushing upwards liquid plugs towards the condenser. The two-phase fluid then enters a Liebig condenser in which the vapor is condensed at constant temperature with a water flow at 25 °C. The condensate return to the evaporator by gravity and the cycle starts over.

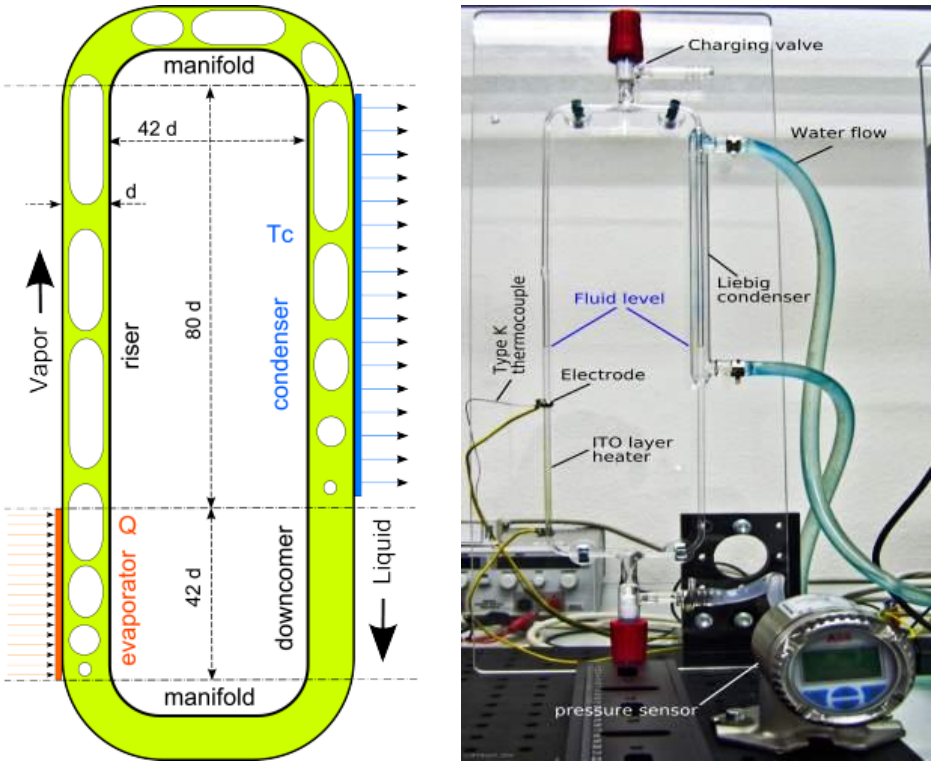

Fig. 1. Thermosyphon principle (left) and experimental setup (right)

The closed loop thermosyphon was manufactured out of 2.4 mm diameter borosilicate glass. The thermosyphon is equipped with a 100 nm semi-transparent Indium Titanium Oxide layer as a direct current heating evaporator. The internal pressure was measured through a valve on the bottom of the loop. A second valve at the top was used to change the filling of the thermosyphon. The electrical current was applied through two electrodes clamped on a silver padding which was applied on a 2.5 mm long section of the Indium Titanium Oxide layer at the bottom and top of the evaporator. A type K thermocouple soldered on the top electrode measured the temperature. The heating power was varied between 5 and 24 W. Two laser-diode beams (1 mW @ 650 nm) were projected through the glass tube and focused with two lenses (focal length:

100 mm) as shown in Fig. 2. After crossing the tube, the laser beams were received by two photodiodes. The resulting voltage signals from the two diodes and the pressure sensor were recorded by a National Instruments SCXI acquisition system. Then, with an appropriate signal processing, it was possible to determine the maximum of the velocity, the length and the frequency of vapor bubbles, the frequency of the thermosyphon cycles for different filling and for several electrical power. The different instruments used for measurements and their accuracy is shown in table 1.

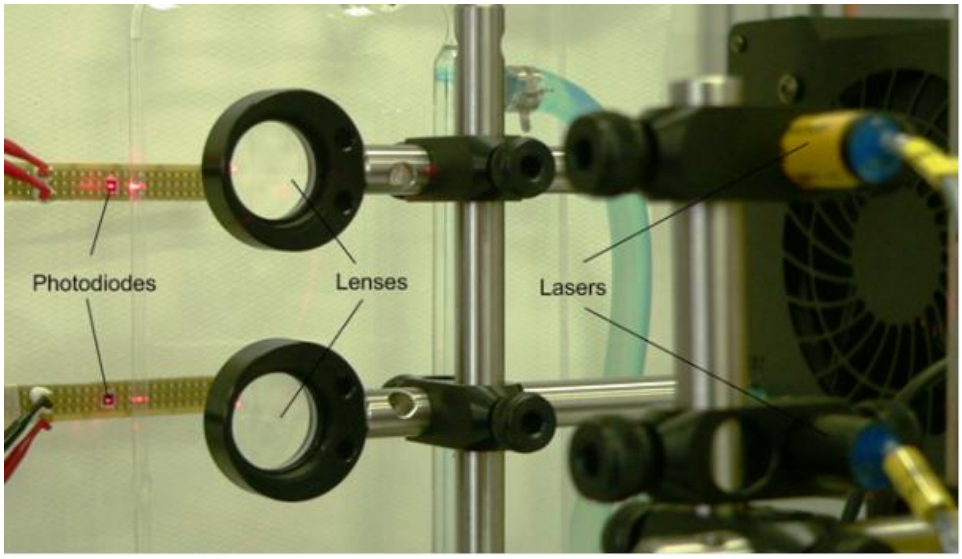

Fig. 2. Picture of the laser diodes arrangement

Table 1. Measuring devices and accuracy

Measurement	Device	Measured range	Accuracy	Unit
Power	**Christ CPM138 wattmeter**	**5–35**	**0.05–0.35**	**W**
Heater temperature	**TC type K + JUMO dieco**	**24–73**	**±1.5**	**°C**
Water temperature	**Alman Reserator XT cooler**	**24–25**	**±1.5**	**°C**
Pressure	**ABB 261AS**	**44–207**	**±1**	**kPa**

MEASUREMENTS ANALYSIS METHOD

The difference in refractive index between liquid and vapor causes the laser beam angle of incidence to change with the passage of a liquid slug or vapor bubble in the tube, resulting in a drop in light intensity detected by the photodiode, thus recording a different voltage signal. The signal obtained using the cross-covariance is characterised by one high amplitude peak, which gives the time delay between the two signals, as shown in Fig. 3. Knowing the distance between the two lasers, it was possible to determine the maximum velocity of the bubbles and liquid slugs. Assuming the velocities of the bubbles and liquid slugs are the same, it is then possible to calculate the fluid mass flow rate. Different number acquisition points were used but beyond 15000 acquisition points there was no influence on the determination of the time delay. For the experiments, the duration of the acquisition chosen was 3–4 min. Measures could be repeated during a week within 5% of error for a same filling of the thermosyphon. The sampling rate was set at 10 kHz.

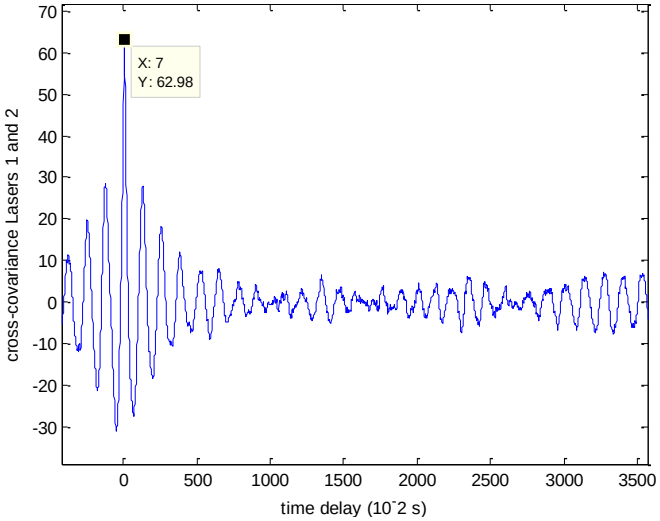

Fig. 3. Cross-covariance signal 1aser 1 and 2 versus time delay (10^{-2} s).

LIMITS OF THE METHOD

This method showed two main limitations:

- coalescence phenomena can cause the signals of the first and second photodiode to be too different. The presence of the coalescence phenomena depends on the flow pattern, hence on the filling of the thermosyphon and the electrical power. This can also happen when a bubble is growing or when its length is decreasing. Backflow of the bubbles in the thermosyphon can also affect adversely the signal. Then a bubble would be counted twice by one of the photodiode.
- If the signal is perfectly periodic (period T), the cross-covariance could indicate a time delay of (t+k·T) because of the periodicity of the signals, k being an integer.

Because of these limitations, the distance between the two couple laser beams/photodiode had to be optimized. If the distance is too high, coalescence phenomena, growth or decrease in length of the bubbles will be detected by the photodiodes. If the signal is too periodic the distance between the two photodiodes should be lower than the flow velocity multiplied by the signal's period. But if this distance is too low, uncertainties will increase. A good compromise was a distance within 2 cm and 4.5 cm. The cross-covariance method is only applicable for a bubbly/slug flow and slug/semi-annular flow, thus measurements were impossible for a higher heating power than 15 W or for a less filling than 50%.

CALCULATION OF BUBBLE VELOCITY

The void fraction depends on the length of the bubbles and on the length of the liquid plugs. If the instantaneous velocities of the vapor and of the liquid are the same (homonegeous model) and are equal to the velocity U given by the cross-covariance's method, the void fraction can be written as a function of the crossing time of the couple photodiode/laser beam by vapor bubbles T_g and by a liquid plugs T_l:

$$\varepsilon = \frac{U.T_g}{(U.T_g + U.T_l)}$$
$$\varepsilon = \frac{T_g}{(T_g + T_l)} \qquad (1)$$

The voltage signals $V(t)$ from the two photodiodes detects the crossing of a couple photodiode/laser beam by a bubble or a liquid plug. For each voltage signal ($V_1(t)$ for laser 1 and $V_2(t)$ for laser 2, shown in Fig. 4 left), a voltage difference $\Delta V_i(t)$, i=1 or 2, can be calculated:

$$\Delta V_i(t) = V_i(t) - V_i(t + \Delta t), \quad (2)$$

Δt being the acquisition time step. This difference voltage is shown in Fig. 4 right and results in a peak each time the flow changes from liquid to vapor and inversely. In order count vapour bubbles and liquid slugs a peak detection threshold was chosen (dashed lines in Fig. 4 right). Thus, the time delay between a consecutive positive peak and negative peak, which is the time delay T_g between the front and back of a bubble can be calculated. The same method was applied to determine T_l. Finally, the void fractions ε_1 and ε_2 for the first and the second photodiode respectively and the average void fraction can be calculated. With the average fluid pressure vapor and liquid densities are known, hence the vapour quality is calculated.

If the threshold was too high, some peaks were not detected and there was insufficient information for calculations. If the threshold was too low, noise signal was considered similar to the peaks due to bubbles or drops. In this study, the ratio signal over noise was around 14. The best choice was 0.01 V. These threshold values were kept for each experimental set up.

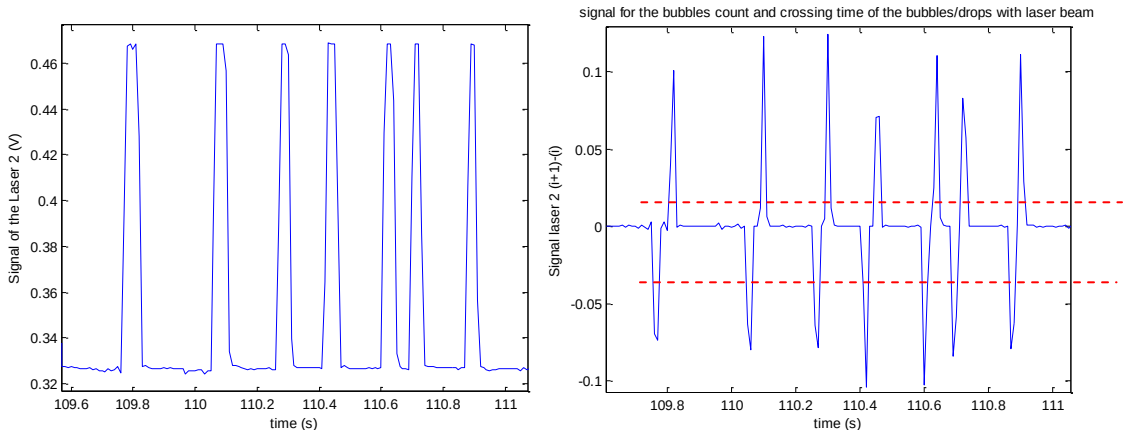

Fig. 4. Left: time series of the signal of the Laser 2 versus time (s). Right: threshold detection applied to the same signal

PRESSURE MEASUREMENTS

The static pressure at the bottom of the thermosyphon was measured with a pressure transducer. The signal was periodic due to the cyclic behaviour of the thermosyphon. A Fast Fourier Transform gave the main frequencies of the pressure signal and the main frequencies of the couples photodiode/laser beam. As shown in Figs. 5 and 6 left, the same value of the cycle frequency was found for all the signals. This frequency increases with the electrical power. For example, frequencies for 80% filling are 0.4 Hz at 5 W and 1.2 Hz at 23 W. A fitting of the pressure signal confirmed the sinusoidal behaviour of the pressure as shown in Fig. 6 right.

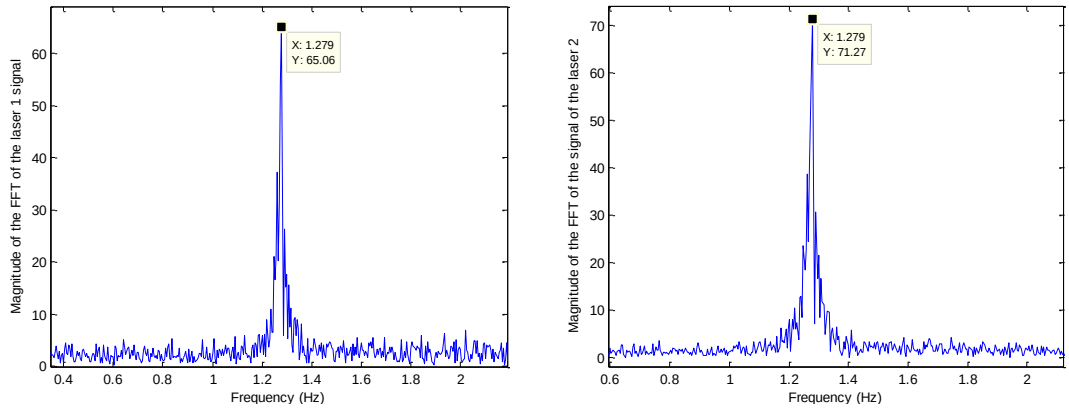

Fig. 5. Left: FFT of the Laser 1 signal. Right: FFT of the Laser 2 signal

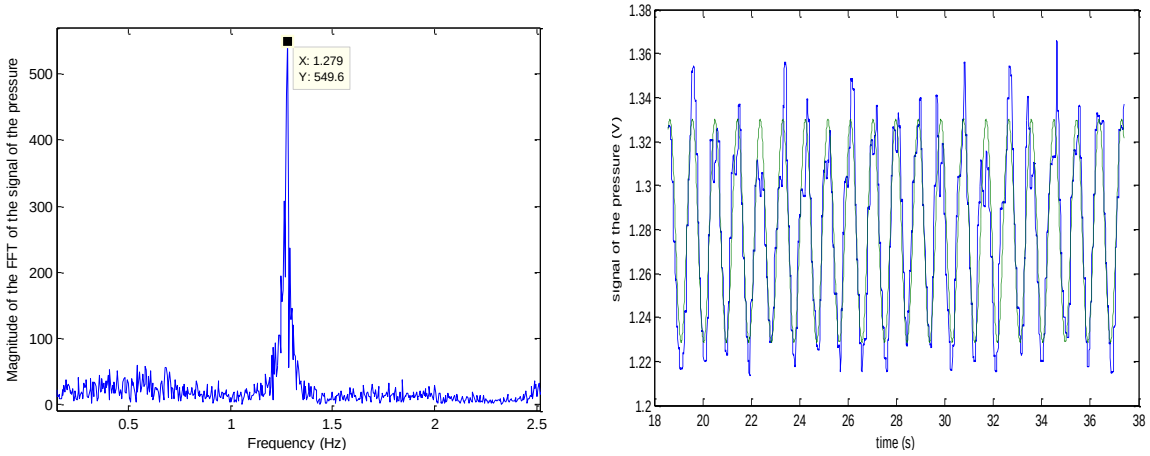

Fig. 6. Left: FFT of the pressure signal. Right: time series of pressure signal (V) and fit function; dashed line: 1.52 + 0.04 sin(6.73*t* +1.7)

RESULTS

Fig. 7 shows the total mass flow rate versus the heating power for various fillings of the thermosyphon (left) and the total mass flow rate versus filling for various heating powers (right). As expected the mass flow increases to a maximum and decreases, both with power or with the thermosyphon filling. At 84% filling however the mass flow always increases with power, but it is suspected that a maximum would be reached at a higher power that was not possible to generate with the present setup.

A thermosyphon model based on the simultaneous solving of the three conservation equations with a minimization algorithm was presented by Agostini and Habert [9] and compared to the present measurements in Fig. 8. The agreement between simulations and measurements is quite dependant on the filling ratio, the best agreement being obtained for filing ratios favoring the elongated bubble flow regime. For low (52%) and high (80% not shown here) filling ratio the agreement is not as good as for 67%. However the trend and order of magnitude of the mass flow rate are adequately predicted by this simple one dimensional model.

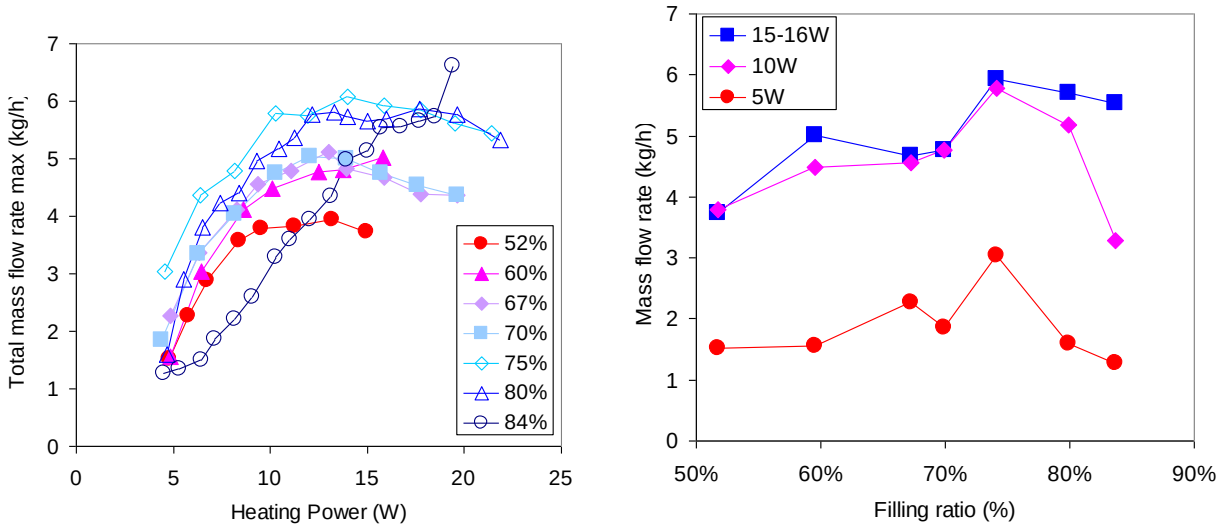

Fig. 7. Left: total mass flow rate maximum (kg/h) versus heating power (W). Right: total mass flow rate maximum (kg/h) versus filling (%)

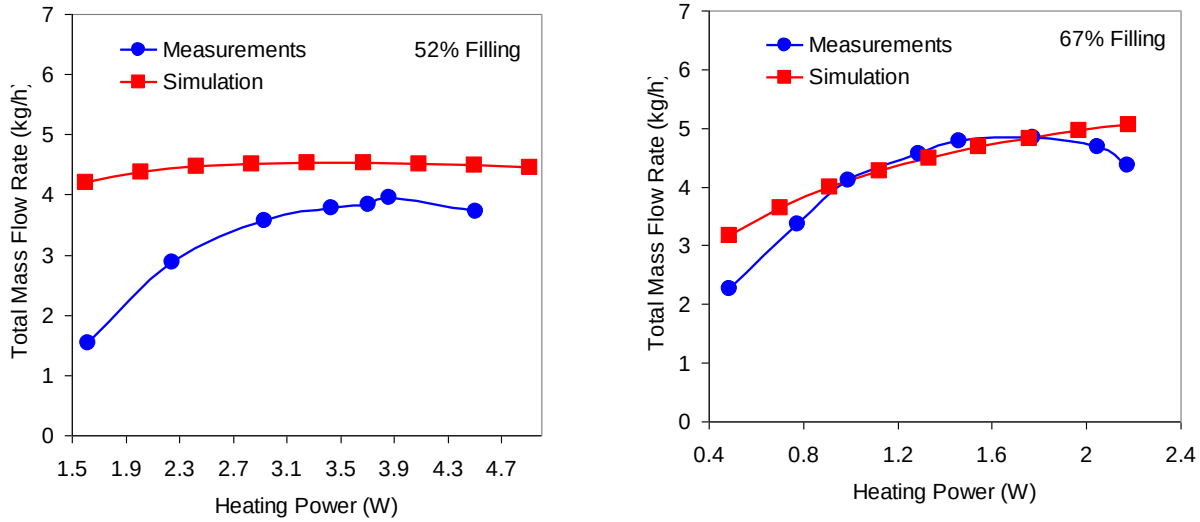

Fig. 8. Comparison between the experimental and the simulated total mass flow rates versus heating power for 52% (right) and 67% filling (left)

CONCLUSIONS

A non intrusive optical mass flow measurement method for a transparent small channel thermosyphon was presented. Based on the use of two sets of laser beam and photodiodes, this method does not add any pressure drop to the system, but is limited to the elongated flow regime. These measurements showed that the mass flow exhibits a maximum with heat load and fluid filling ratio, which is expected in bubble pump systems. Furthermore the trend and order of magnitude of the mass flow rate were found to be adequately predicted by a one dimensional thermosyphon model based on the three conservations equations. The next step will be to measure the temperature distribution on the evaporator with an infrared camera et correlate it to the bubble frequency.

NOMENCLATURE

ε	Void fraction	(-)
x	Vapor quality	(-)
T	Thermosyphon cycle period	(s)
T_g	Mean crossing time of bubbles	(s)
T_l	Mean crossing time of liquid slugs	(s)
Δt	Time delay between two acquisitions	(s)
U_g	Velocity of the gas flow	(m/s)
U_l	Velocity of the liquid flow	(m/s)
U	Maximum velocity of the fluid	(m/s)
V	Voltage signal from the photodiode	(V)
ΔV	Voltage difference	(V)

References

1. Vasiliev L. L. State-of-the-art on heat pipe technology in the former soviet union // *Appl. Therm. Eng*. 1998. Vol. 18, No. 7. Pp. 507–551.
2. Delano N. *Design Analysis of the Einstein Refrigeration Cycle* // PhD thesis, Georgia Institute of Technology, June 1998.

3. Nayak A., Lathouwers D., van der Hagen T., Schrauwen F., Molenaar P., Rogers A. A numerical study of boiling flow instability of a reactor thermosyphon system // *Appl. Therm. Eng.* 2006. Vol. 26. Pp. 644–653.
4. Khodabandeh R. Heat transfer in the evaporator of an advanced two-phase thermosyphon loop // *Int. J. of Refrigeration*. 2008. Vol 28. Pp. 190–202.
5. Khodabandeh R., Pressure drop in riser and evaporator of an advanced two-phase thermosyphon loop // *Int. J. of Refrigeration*. 2005. Vol. 28. Pp. 725–734.
6. Ong K., Haider-E-Alahi M. Performance of a R-134-a-filled thermosyphon // *Appl. Therm. Eng*. 2003. Vol. 23. Pp. 2373–2381.
7. Nayak A., Lathouwers D., van der Hagen T., Schrauwen F., Molenaar P., Rogers A. A numerical study of boiling flow instability of a reactor thermosyphon system // *Appl. Therm. Eng*. 2006. Vol. 26. Pp. 644–653.
8. MacDonald T., Hwang K., Diciccio R. Thermosyphon loop performance characteristics: Part 1. Experimental Study // *ASHRAE Trans*. 1997. Vol. 83. No. 2467. Pp. 250–259.
9. Agostini B., Habert M. Measurement of the performances of a transparent closed loop two-phase thermosyphon // *Proc. of the Advanced Computational Methods and Experiments in Heat Transfer XI, WIT Press publishes leading books in Science and Technology*, 2010. Pp. 227–235.